



Interleukin-35 attenuates blood-brain barrier dysfunction caused by cerebral ischemia-reperfusion injury through inhibiting brain endothelial cell injury

Lei Qian^{1#}, Ming Li^{1#}, Xin Lin^{2#}, Hongwei Teng³, Lulu Yu¹, Maorong Jiang^{4,5}

¹Department of Laboratory Medicine, Binhai County People's Hospital, Binhai, China; ²Department of Clinical Laboratory, Nanjing First Hospital, Nanjing Medical University, Nanjing, China; ³Department of Neurosurgery, Binhai County People's Hospital, Binhai, China; ⁴Key Laboratory of Neuroregeneration of Jiangsu and Ministry of Education, Jiangsu Clinical Medicine Center of Tissue Engineering and Nerve Injury Repair, Co-Innovation Center of Neuroregeneration, Nantong University, Nantong, China; ⁵School of Life Sciences, Nantong University, Nantong, China

Contributions: (I) Conception and design: L Qian; (II) Administrative support: M Jiang; (III) Provision of study materials or patients: L Qian; (IV) Collection and assembly of data: X Lin, M Li; (V) Data analysis and interpretation: All authors; (VI) Manuscript writing: All authors; (VII) Final approval of manuscript: All authors.

[#]These authors contributed equally to this work.

Correspondence to: Maorong Jiang. Key Laboratory of Neuroregeneration of Jiangsu and Ministry of Education, Jiangsu Clinical Medicine Center of Tissue Engineering and Nerve Injury Repair, Co-Innovation Center of Neuroregeneration, Nantong University, Nantong, China; School of Life Sciences, Nantong University, Nantong, China. Email: jiangmr@ntu.edu.cn.

Background: Interleukin-35 (IL-35), an anti-inflammatory and antioxidant cytokine, plays a potent immunosuppressive role in various diseases. However, the effects of IL-35 on blood-brain barrier (BBB) dysfunction in ischemic stroke are not well characterized.

Methods: A total of 150 male C57BL/6 mice (aged 6–8 weeks and weighing 20–25 g) were used in this study. The protective effects of IL-35 against BBB dysfunction were examined using a mouse model of middle cerebral artery occlusion (MCAO) and an *in vitro* model of oxygen-glucose deprivation/reoxygenation (OGD/R) injury in mouse brain endothelial cells (bEnd.3).

Results: Intracerebroventricular administration of IL-35 (10 µg/g) was found to reduce cerebral edema and Evans blue (EB) leakage, and increase the expression of tight junction (TJ) proteins, thereby attenuating MCAO-induced neurological deficit in mice. Moreover, IL-35 (20 ng/mL) treatment upregulated the expression of TJ proteins in OGD/R-induced bEnd.3 cells. IL-35 also markedly suppressed the expression of caspase-1, IL-1β, and gasdermin D (GSDMD) *in vivo* and *in vitro*. In addition, IL-35 decreased the generation of reactive oxygen species (ROS) and inhibited the expression of thioredoxin-interacting protein (TXNIP) in OGD/R-induced bEnd.3 cells.

Conclusions: These results indicated that IL-35 exerts a protective effect on the BBB by targeting the ROS/TXNIP/caspase-1 pathway in cerebral ischemia-reperfusion (I/R) injury.

Keywords: Ischemic stroke; interleukin-35 (IL-35); blood-brain barrier (BBB); caspase-1

Submitted May 07, 2022. Accepted for publication Jun 28, 2022.

doi: 10.21037/atm-22-2770

View this article at: <https://dx.doi.org/10.21037/atm-22-2770>

Introduction

Ischemic stroke is caused by cerebral vascular occlusion, resulting in decreased blood flow to brain tissue (1). The condition is associated with significant morbidity and

mortality (2). The decreased oxygen and glucose levels in the brain trigger impairment of the blood brain barrier (BBB) and neuronal cell death via activation of oxidative stress signaling and production of inflammatory and

cytotoxic molecules (3,4). Furthermore, post-ischemic reperfusion, which can occur following treatment with recombinant tissue plasminogen activator or thrombectomy, accelerates the production of reactive oxygen species (ROS) and inflammation in ischemic tissues, leading to ischemia-reperfusion (I/R) injury (5,6). Notably, I/R impairs the reactivity of the cerebral microvascular endothelium and triggers BBB dysfunction, thereby reducing the efficacy of related arterial recanalization (7,8). However, currently, there is a paucity of effective strategies to protect the integrity of the BBB in the setting of brain ischemia.

Inflammasomes are composed of cytosolic multiprotein complexes that, when assembled, lead to the activation of caspases and the subsequent cleavage of pro-interleukin (IL)-18, pro-IL-1 β , and gasdermin D (GSDMD) into their respective mature forms, namely, IL-18, IL-1 β , and the N-domain of GSDMD (GSDMD-NT) (9). Consequently, GSDMD-NT can mediate the formation of membrane pores and eventually release inflammatory mediators into the extracellular tissue, causing a severe inflammatory reaction (10,11). Of note, emerging evidence indicates that inflammasomes facilitate the disruption of the BBB after cerebral ischemia and reperfusion (12). Consistent with this, inhibition of inflammasomes was shown to reduce post-ischemic BBB damage, which was related to the upregulated expression of tight junction (TJ) proteins zonule occlusion-1 (ZO-1) and occludin (13,14). Mechanistically, activation of inflammasomes after cerebral ischemia is related to many factors, such as the ROS and thioredoxin-interacting protein (TXNIP) pathways (15-17). Therefore, inhibiting the generation of ROS and TXNIP expression in endothelial cells (ECs) may reduce the activation of inflammasomes, and this may represent a novel therapeutic strategy for patients with ischemic stroke.

Cytokines are small polypeptides, normally expressed at very low levels, which regulate immune responses. Various cytokines can either mediate the inflammatory response or act as anti-inflammatory molecules, which terminate the inflammatory response. IL-35, an anti-inflammatory and antioxidant cytokine, has a protective effect against vascular EC damage (18). For example, in the mouse sepsis model, IL-35 has been shown to inhibit lipopolysaccharide-induced EC activation via the mitogen-activated proliferation protein kinase (MAPK)-activated protein 1 (AP-1)-mediated inflammatory pathway (19). Moreover, in apolipoprotein E (ApoE) knockout mice, IL-35 inhibited EC activation induced by lysophosphatidylcholine via reducing the production of mitochondrial ROS, thereby inhibiting the

development of atherosclerotic lesions (20). In our previous research, we demonstrated that IL-35 inhibited the production of ROS by human umbilical vein ECs induced by the serum of preeclampsia patients by up-regulating the expression of S100A8 protein, thereby inhibiting apoptosis of human umbilical vein ECs (21). Importantly, the beneficial effects of IL-35 on the neurological function of mice with cerebral ischemia are believed to be mainly attributed to its anti-inflammatory activities (22). However, the potential protective effects of IL-35 against BBB dysfunction in cerebral ischemia and the associated underlying mechanisms are not well characterized.

This current study investigated whether IL-35 indeed protects against BBB dysfunction caused by cerebral ischemia, and if so, whether treatment with IL-35 can attenuate the activation of caspase-1. The effects of IL-35 treatment on BBB dysfunction were examined in a mouse model of transient middle cerebral artery occlusion (MCAO) and in an *in vitro* model of oxygen-glucose deprivation and reperfusion (OGD-R) in brain ECs. In addition, since generation of ROS is a common upstream mechanism implicated in caspase-1 activation, the role of IL-35 on the ROS/TXNIP/caspase-1 signaling pathway was also investigated. We present the following article in accordance with the ARRIVE reporting checklist (available at <https://atm.amegroups.com/article/view/10.21037/atm-22-2770/rc>).

Methods

Establishment of the MCAO model

All animal experiments were approved by the Experimental Animal Ethics Committee of Nantong University (Permission No. 2019012) and performed according to *The Guide for the Care and Use of Laboratory Animals* (National Institutes of Health Publication). A protocol was prepared before the study without registration. Male C57BL/6 mice (aged 6–8 weeks and weighing 20–25 g) were purchased from the experimental animal center of the Nanjing University (Nanjing, China). Overnight-fasted mice were subjected to MCAO as previously described (23). Briefly, mice were anesthetized by intraperitoneal injection of 4% chloral hydrate (0.1 mL/10 g body weight) and a neck incision was made to expose the left common carotid artery bifurcation. The left external carotid artery was then ligated and a 6-0 nylon monofilament suture (RWD Life Science, Shenzhen, China) was inserted into the left internal carotid artery for a distance of 9–10 mm to block the left middle

cerebral artery. One hour after occlusion, the suture was withdrawn. Mice in the sham group were subjected to the same manipulation, but without inserting a suture. All animals were maintained in a controlled environment (12-hour light/dark cycle; 24 ± 2 °C) with free access to standard laboratory food and filtered clean water.

Experimental design and treatment

Mice were randomly divided into three groups: (I) the sham group; (II) the MCAO group; and (III) the MCAO + IL-35 group. Recombinant mouse IL-35 (St. Louis, MO, USA, America) was diluted with phosphate buffered saline (PBS) and administered to animals in the MCAO + IL-35 group at 10 µg/g body weight (24) via intracerebroventricular (i.c.v) injection into the parietal region (0.5 mm posterior, 1.0 mm right lateral, and 2.5 mm deep to the Bregma) at 1 hour and 24 hours after reperfusion. Mice in the sham and MCAO groups were administered the same volume of PBS (*Figure 1A*).

A total of 150 mice were used for this study. There were 18 mice in each experiment ($n=6$ /group). For the evaluation of neurological deficit, 8 mice were used per group as follows: (I) Fluoro-Jade C (FJC) staining; (II) infarct volume assessment; (III) Evans blue (EB) staining; (IV) brain water content; (V) Western blotting; (VI) immunofluorescence analysis; and (VII) enzyme-linked immunosorbent assay (ELISA). Mice that died before sampling could be conducted ($n=21$) were excluded from the total numbers. All researchers conducting animal testing were blinded to the treatment conditions.

FJC staining

Mice were anesthetized 24 hours after reperfusion and perfused with 0.9% saline. The brain tissue was kept in 4% paraformaldehyde (PFA) solution at 4 °C overnight. Selected brain coronal slices (bregma -1 to +1 mm) were cut into 16-mm coronal sections using a Leica VT1000 S vibratome (Leica Microsystems AG, Nussloch, Germany) and stained with FJC (Biosensis, Thebarton, Australia) according to the manufacturer's instructions. Two non-overlapping images of each brain slice were taken. FJC-positive neurons were observed with ImageJ software (ImageJ 1.5, NIH, USA) to measure the degree of neuronal degeneration and the data are presented as cells/mm².

Evaluation of neurological deficit

After MCAO and 2 days of reperfusion, neurological deficit

in the experimental animals was assessed by a researcher blinded to the study design according to the Garcia scoring method (25). Briefly, the assessment included 6 tests: (I) spontaneous activity; (II) forepaw outstretching; (III) symmetry in the movement of four limbs; (IV) body proprioception; (V) response to vibrissae touch; and (VI) climbing. Each of these assessments was graded using a scale of 0–3. The higher the evaluated score, the less the neurological deficit.

Infarct volume assessment

Infarct volume was assessed by 2,3,5-triphenyltetrazolium chloride (TTC) (Yi Fei Xue Biotechnology, Nanjing, China) staining after 24 hours of reperfusion, as previously described (26). Briefly, after mice were sacrificed, the brains were quickly harvested, sliced into continuous coronal sections (2 mm thick), and treated with 2% TTC phosphate buffer for 10 minutes at 37 °C. Sections were then placed in PFA phosphate buffer (4%) for 30 minutes. An electronic scanner (Tsinghua Unisplendour A688, Xi'an, China) and a multimedia image analysis system (Image-Pro Plus6.0, Media Cybernetics, Wyoming, USA) were used to calculate the ratio of infarct tissue (white) to the total volume of the slice. The proportion of infarct volume = infarct area (while pale area)/total area of slice $\times 100\%$.

BBB permeability

BBB permeability was measured by the leakage of EB (St. Louis, MO, USA) into the brain after intravenous injection at 24 hours after reperfusion (23). In brief, normal saline containing EB dye (2%) was injected through the tail vein at a volume of 0.1 mL/10 g body weight and allowed to circulate for 1 hour. The mice were then anesthetized and sacrificed. The ipsilateral hemispheres were removed and homogenized in trichloroacetic acid (1 mL), followed by centrifugation at 12,000 g for 20 minutes. The supernatant was collected and the EB absorbance was measured using a spectrophotometer at 620 nm (Cloud-Clone Corp, TX, USA). The data are presented as microgram of EB per gram of brain tissues. In addition, brain water content was determined 24 hours after reperfusion using the wet-dry method (27). The brains were removed and sliced. The samples were weighed to obtain the total weight (TW) and then placed in an oven for 24 hours at 100 °C to obtain the dry weight (DW). Brain water content was calculated as $[(TW - DW)/TW] \times 100\%$.

Immunofluorescence analysis

For immunofluorescence staining, mice were perfused with PBS after 24 hours of reperfusion and brain coronal slices (bregma -3 to +2 mm) were rapidly post-fixed in 30% sucrose-PFA for 24 hours. Subsequently, 15- μ m sagittal sections were permeabilized with 0.1% Triton-X/PBS, followed by blocking with 10% fetal calf serum and 5% bovine serum albumin (BSA) in PBS for 1 hour. Slides were incubated with primary antibodies against ZO-1, occludin, CD31, caspase-1, and GSDMD (1:400, 1:400, 1:500, and 1:500, respectively; Abcam, Cambridge, MA, USA). Samples were incubated with a secondary antibody (dilution 1:2,000, Yi Fei Xue Biotechnology, Nanjing, China). Nuclei were stained with DAPI for 10 minutes. Finally, sections were photographed and visualized with a Leica fluorescence microscope (Leica, Wetzlar, Germany). Two brain slices per sample were used and two images were taken for each slice.

ELISA

At 24 hours after reperfusion, cortical tissues (100 mg) in the peri-infarct area (bregma -3 to +2 mm) were collected and homogenized with cold PBS in a ratio of 1:9 at below 4 °C. Samples were centrifuged at 430 g for 10 minutes and the supernatant was collected. The concentrations of IL-18 and IL-1 β in the samples were determined using ELISA kits in accordance with the manufacturer's instructions (Yi Fei Xue Biotechnology, Nanjing, China).

Establishment of OGD/R model and drug treatment

Brain endothelial cells (bEnd.3) (Procell Life Science and Technology Co. Ltd., Wuhan, China) were treated with 20 ng/mL IL-35 (21) for 4 hours before and during exposure to OGD/R, which is an accepted *in vitro* model of I/R injury (28). Briefly, cells were cultured in Dulbecco's Modified Eagle Medium (DMEM; Gibco, Carlsbad, CA, USA) containing fetal calf serum (FCS, 10%) and glucose (4.5 g/L) for 24 hours at 37 °C under 5% CO₂. Subsequently, cells were incubated in DMEM without glucose and serum at a density of 1 \times 10⁶ cells/well inside a hypoxia chamber (H35; Don Whitley Scientific Ltd., Shipley, UK) containing 5% CO₂ and 95% N₂ at 37 °C for 18 hours. Thereafter, cells were cultured in normal conditions for 20 hours. Control cells were cultured with standard media in normal conditions. At the end of the experiment, cells were harvested for the further assays.

Detection of ROS and malondialdehyde (MDA)

The bEnd.3 cells (1 \times 10⁵ cells/mL) were cultured in a 6-well plate and treated with IL-35 (20 ng/mL) for 1 hour, followed by exposure to OGD/R insult. Intracellular ROS production was measured using the 2'-7'-dichlorofluorescein diacetate (DCFH-DA) assay kit (Dojindo Laboratories, Kumamoto, Japan) according to the manufacturer's instructions. DCF fluorescence intensity was measured using a microplate reader (1420 VICTOR2, Perkin Elmer Wallac) and observed on a fluorescence microscope (BX-60; Olympus, Tokyo, Japan) at \times 200 magnification. The MDA concentration in cell lysates was determined using a commercial assay kit (Dojindo Laboratories, Kumamoto, Japan) in accordance with the manufacturer's protocols.

Western blot analysis

After the designated treatment, cortical tissues in the peri-infarct region (bregma -3 to +2 mm) and bEnd.3 cells were collected. The total protein was extracted using RIPA lysis buffer. Protein samples (30 μ g) were separated by sodium dodecyl sulfate-polyacrylamide gel electrophoresis (SDS-PAGE; Bio-Rad, Hercules, CA, USA) and transferred to polyvinylidene fluoride (PVDF) membranes. After blocking with 5% nonfat dry milk, the membranes were incubated overnight with primary antibodies against ZO-1, occludin, cleaved caspase-1, GSDMD, and TXNIP (1:1,000, Santa Cruz Biotechnology, Dallas, TX, USA), or β -actin (1:5,000, Yi Fei Xue biotechnology, Nanjing, China). Samples were subsequently incubated with a secondary antibody for 1 hour (dilution 1:10,000, Yi Fei Xue Biotechnology, Nanjing, China). Densitometric measurements were performed using the ChemiDoc™ MP System (Bio-Rad, Hercules, CA, USA).

Statistical analysis

Statistical analyses were conducted using GraphPad Prism version 5.0 (GraphPad Software Inc., San Diego, CA, USA). One-way analysis of variance (ANOVA) followed by Tukey post hoc test was used for multi-group comparisons. In the animal experiments, 6 mice were required in each group to statistically detect a 2.3-fold change (effect size, 90% power) in two-tailed Student's *t* test with a significance level of 5%. Student's *t* tests were performed for comparison between two groups. Two-tailed P values <0.05 were considered statistically significant.

Results

IL-35 treatment alleviated MCAO-induced neurological impairment

To investigate the protective effect of IL-35 against cerebral I/R injury, IL-35 (10 µg/g) was administered (i.c.v) at 1 hour and 24 hours after reperfusion (Figure 1A). TTC staining at 24 hours after reperfusion revealed that there was no infarction in the sham group. However, the infarct volume in the MCAO group was significantly greater than that in the sham group ($P < 0.05$, Figure 1B,1C). Interestingly, the infarct size in the MCAO + IL-35 group was significantly lower than that in the MCAO group ($P < 0.05$, Figure 1B,1C). Furthermore, mice subjected to MCAO injury showed decreased neurological scores compared to those in the sham group. Mice in the MCAO + IL-35 group showed significant improvement in neurological function after I/R compared to the MCAO group ($P < 0.01$, Figure 1D).

Pathologic changes in ischemic stroke are mainly observed in the cortex of the peri-infarct area. Therefore, FJC staining was performed to evaluate the degenerate neurons in the cortex of the peri-infarct area. The number of FJC-positive neurons in the MCAO + IL-35 mice was significantly lesser than that in the MCAO group ($P < 0.01$, Figure 1E-1G). All these findings suggested a neuroprotective effect of IL-35 in MCAO mice.

IL-35 treatment improved MCAO-induced BBB permeability

Previous research has demonstrated the importance of the BBB in ensuring proper neuronal function (29). The ability of IL-35 to improve MCAO-induced neurological function by preventing impairment to the BBB was investigated. At 24 hours after reperfusion, the EB extravasation in MCAO + IL-35 mice was significantly attenuated compared to the MCAO group ($P < 0.05$, Figure 2A). A similar phenomenon was observed with respect to brain water content (Figure 2B).

The expression of TJ proteins ZO-1 and occludin was assessed to determine BBB integrity at 24 hours after reperfusion. Western blot analysis indicated that IL-35 treatment preserved the expression of ZO-1 and occludin in the ischemic brain (Figure 2C-2E). Immunofluorescence staining was performed to determine the ZO-1 and occludin expression in vascular ECs in the peri-infarct cortex. There was serious damage to the two TJ proteins distributed in the cerebral microvessels, while MCAO + IL-35 mice showed

significantly higher expression of ZO-1 and occludin in vascular ECs compared with the MCAO group (Figure 2F,2G). Collectively, these results demonstrated that IL-35 exerted a potent protective effect on the BBB in mice with stroke.

IL-35 inhibited caspase-1 activity in MCAO-induced BBB injury

Caspase-1 has been demonstrated to be related to BBB injury (30). To biochemically assess the effect of IL-35 on caspase-1, the expression of cleaved caspase-1, IL-1 β , IL-18, and GSDMD was examined in the peri-infarct cortex at 24 hours after reperfusion. Western blot analysis showed a dramatic increase in the expression of GSDMD and cleaved caspase-1 in the MCAO group compared to the sham group ($P < 0.05$, Figure 3A-3C). However, the MCAO + IL-35 group showed significantly lower expressions of cleaved caspase-1 and GSDMD protein in the ischemic cortex compared to the MCAO group ($P < 0.05$, Figure 3A-3C). In addition, ELISA analysis indicated significantly lower amounts of IL-1 β and IL-18 in the cortical tissues in the MCAO + IL-35 group compared with the MCAO group ($P < 0.05$, Figure 3D,3E).

Cleaved caspase-1 and GSDMD expression could be observed in vascular ECs in brain slices in the immunofluorescence colocalization experiments. The images showed that IL-35 treatment decreased the expression of cleaved caspase-1 and GSDMD in vascular ECs (vs. MCAO, Figure 3F,3G). These results suggested that IL-35 may alleviate BBB injury by inhibiting the activation of caspase-1 in vascular ECs.

IL-35 treatment alleviated OGD/R-induced bEnd.3 cells injury

The effects of IL-35 on bEnd.3 cells injured under OGD/R were investigated. Western blot results showed that IL-35 treatment reduced the elevated expression of GSDMD and cleaved caspase-1 in bEnd.3 cells subjected to OGD/R (Figure 4A-4C) and dramatically decreased the levels of IL-1 β and IL-18 in the culture supernatant (vs. OGD/R cells, $P < 0.05$, Figure 4D,4E). Moreover, the protein levels of ZO-1 and occludin were downregulated in bEnd.3 cells subjected to OGD/R, while IL-35 treatment restored the expression of ZO-1 and occludin (Figure 4F-4H). These results showed that IL-35 treatment alleviated bEnd.3 cell injury in response to OGD/R.

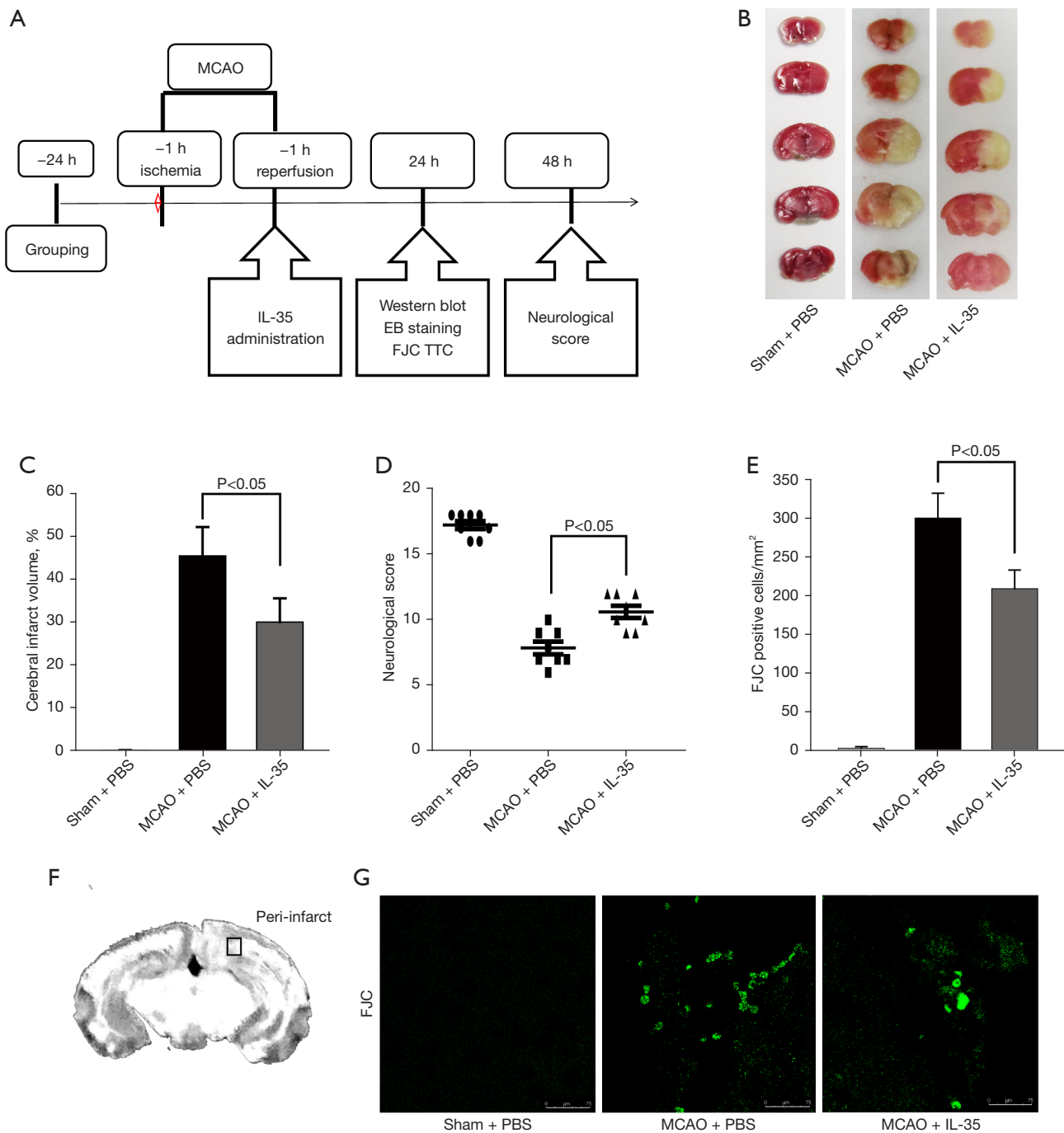


Figure 1 IL-35 treatment ameliorated I/R-induced cerebral infarction and neurological deficit. (A) Experimental protocol in mice subjected to MCAO. IL-35 (10 $\mu\text{g/g}$) was administered at 1 hour and 24 hours after reperfusion by intracerebroventricular injection. (B,C) Representative images and statistical analysis of the infarct areas. The infarct volume was quantified using TTC staining at 24 hours after ischemia ($n=6$ per group). (D) Neurological scores at 48 hours after reperfusion according to the Garcia scoring method ($n=8$ per group). (E-G) Representative images and statistical analysis of neuronal degeneration. FJC staining was performed 24 hours after I/R (scale bar: 75 μm). Data are presented as mean \pm SD ($n=6$ per group). MCAO, middle cerebral artery occlusion; IL, interleukin; EB, Evans blue; FJC, fluoro-Jade C; TTC, 2,3,5-triphenyltetrazolium chloride; PBS, phosphate buffered saline; I/R, ischemia/reperfusion; SD, standard deviation.

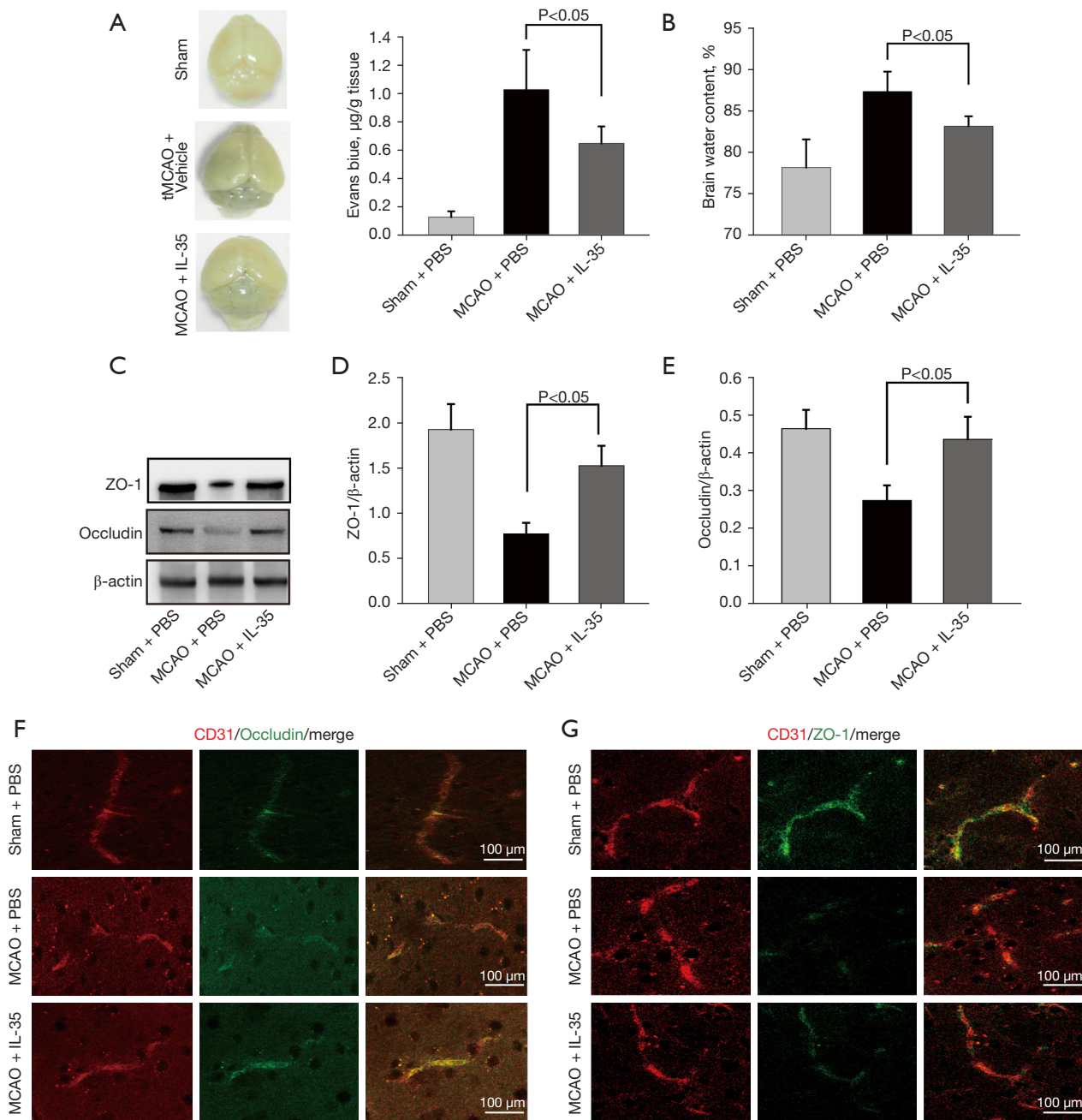


Figure 2 IL-35 suppressed I/R-induced BBB dysfunction. MCAO mice were administered IL-35 (10 $\mu\text{g/g}$) or PBS until sacrificed. (A) Representative images and statistical analysis of EB leakage analysis at 24 hours after reperfusion. (B) Brain water content analysis of the injured hemisphere at 24 hours after reperfusion. (C-E) Western blot images and analysis of ZO-1 and occludin expressions in the peri-ischemic region at 24 hours after reperfusion. Data presented as mean \pm SD (n=6 per group). (F,G) Immunofluorescence staining of ZO-1 and occludin (green) expression in vascular endothelial cells (CD31, red) in MCAO mice brain coronal sections (scale bar: 100 μm ; n=6 per group). MCAO, middle cerebral artery occlusion; IL, interleukin; PBS, phosphate buffered saline; ZO-1, zonula occludens-1; I/R, ischemia/reperfusion; BBB, blood-brain barrier; EB, Evans blue; SD, standard deviation.

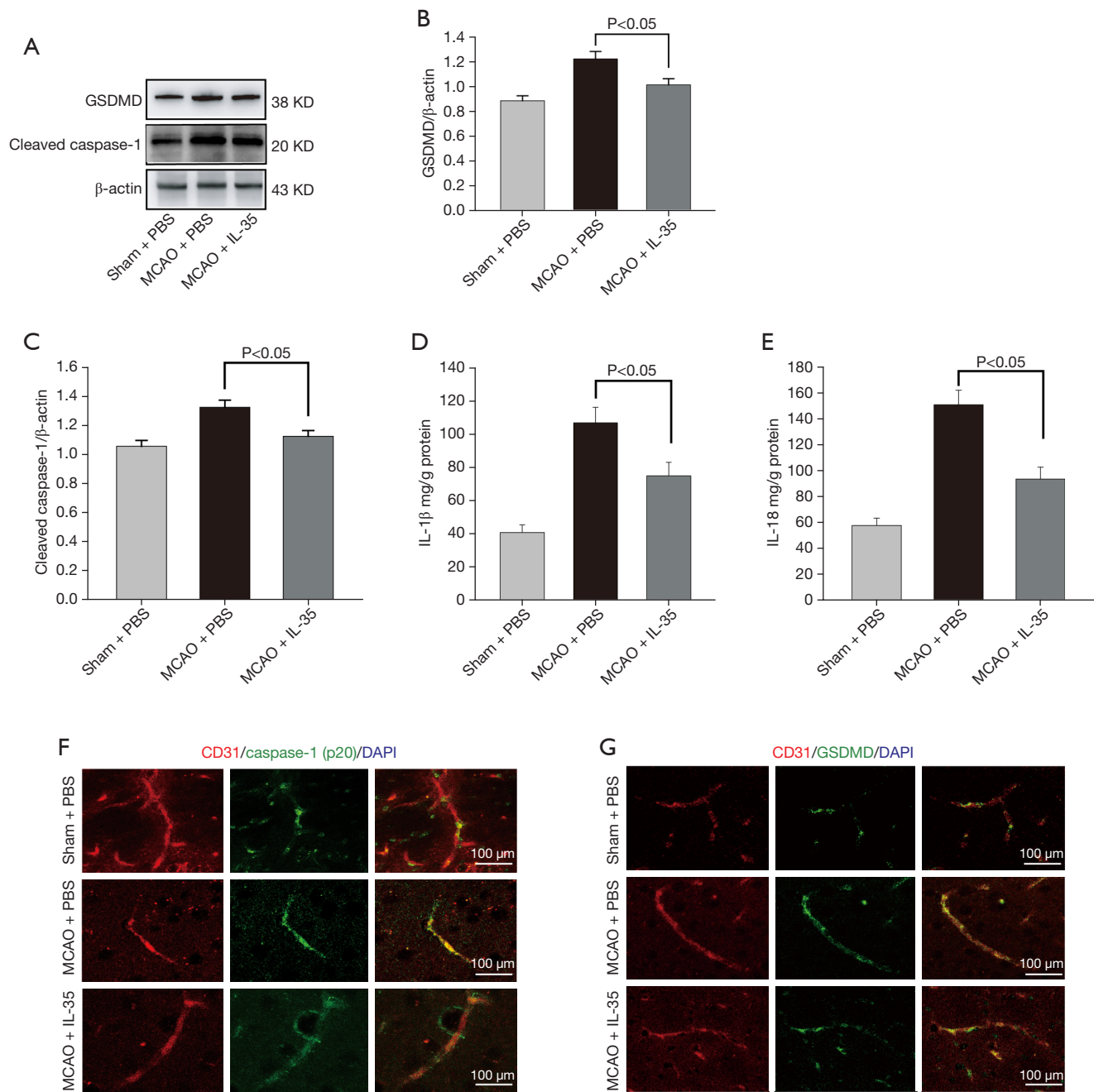


Figure 3 IL-35 suppressed I/R-induced brain tissue injury in the ischemic cortex. MCAO mice were administered IL-35 (10 μg/g) or PBS and sacrificed at 24 hours after reperfusion. (A-C) Western blot images and analysis of cleaved caspase-1 and GSDMD expressions in the peri-ischemic region. Error bars represent mean ± SD; n=6 per group. (D,E) Results of ELISA showing the concentrations of IL-18 and IL-1β in the cortical tissues. Error bars represent mean ± SD; n=6 per group. (F,G) Immunofluorescence staining of cleaved caspase-1 and GSDMD (green) expression in vascular endothelial cells (CD31, red) in the peri-ischemic regions (scale bar: 100 μm; n=6 per group). GSDMD, gasdermin D; PBS, phosphate buffered saline; MCAO, middle cerebral artery occlusion; IL, interleukin; I/R, ischemia/reperfusion; SD, standard deviation; ELISA, enzyme-linked immunosorbent assay.

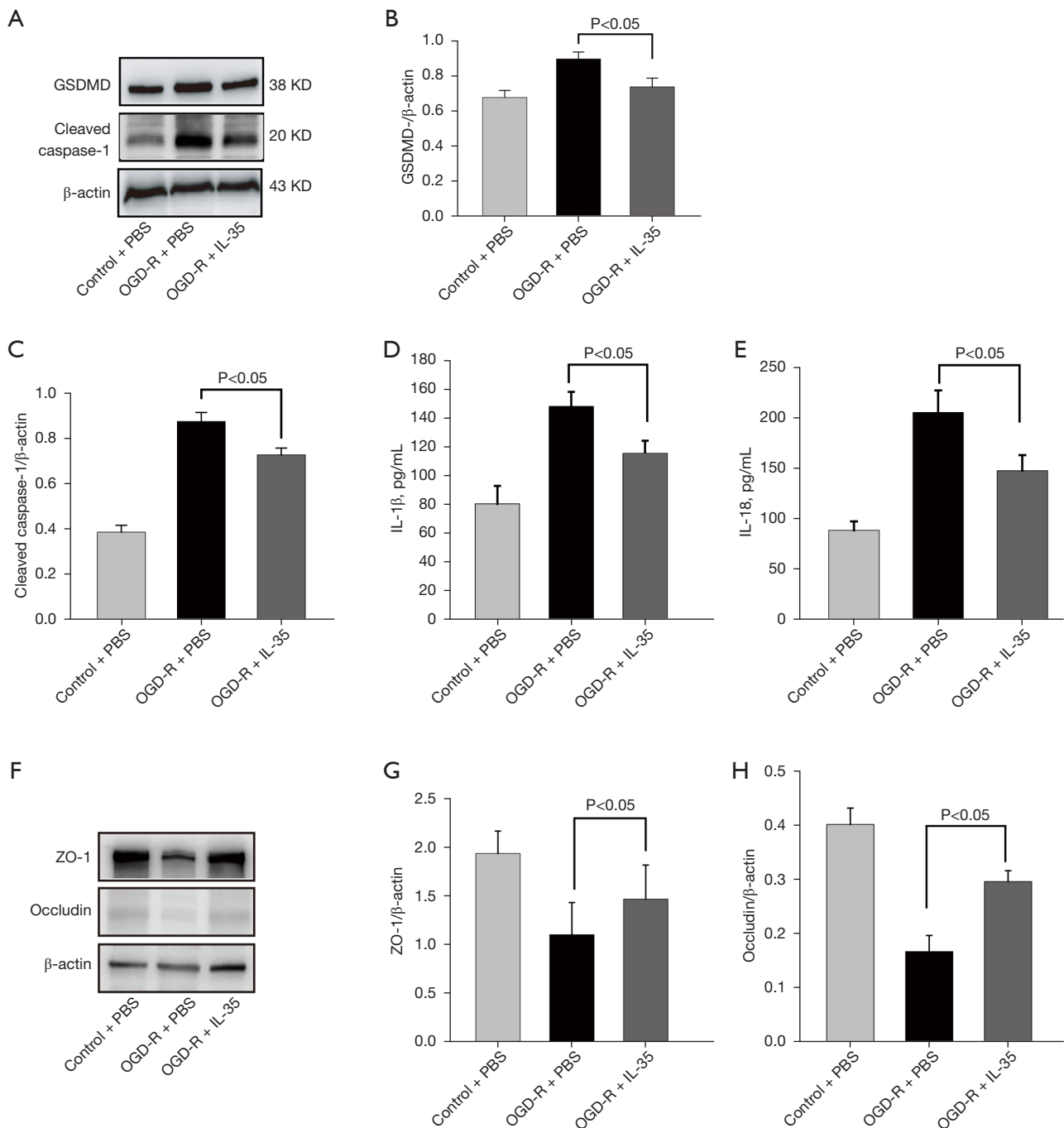


Figure 4 IL-35 protected OGD/R-induced endothelial cell injury. bEnd.3 cells were pretreated with or without IL-35 and then subjected to 6 hours of OGD and 18 hours reoxygenation. (A-C) Western blot images and analysis of cleaved caspase-1 and GSDMD expressions in bEnd.3 cells. (D,E) Results of ELISA showing the levels of IL-18 and IL-1 β in the culture supernatant. (F-H) Results of Western blot assay showing the protein expressions of ZO-1 and occludin in bEnd.3 cells. Error bars represent mean \pm SD of at least three independent experiments. GSDMD, gasdermin D; PBS, phosphate buffered saline; OGD-R, oxygen-glucose deprivation and reperfusion; IL, interleukin; ZO-1, zonula occludens-1; bEnd.3, brain endothelial cells; ELISA, enzyme-linked immunosorbent assay; SD, standard deviation.

IL-35 suppressed the production of ROS in OGD/R-induced bEnd.3 cells

Over-accumulation of free radicals is known to trigger the activation of NLRP3 inflammasome. Due to its antioxidant effects, IL-35 may suppress caspase-1 activation by reducing the levels of ROS. Indeed, the DCFH-DA fluorescence assays demonstrated that treatment with IL-35 reduced the production of ROS in OGD/R-induced bEnd.3 cells (Figure 5A,5B). In addition, IL-35 reduced the concentration of MDA in bEnd.3 cells compared to untreated OGD/R cells ($P < 0.05$, Figure 5C).

Under conditions of high ROS levels, TXNIP has been shown to quickly bind inflammasomes and trigger the assembly of inflammasomes (31). Furthermore, phosphorylation of MAPK has been proposed to upregulate transcription of the inflammasome components (32). Therefore, the effects of IL-35 on p38 MAPK and TXNIP expression was examined in bEnd.3 cells subjected to OGD/R. Western blot analysis showed that IL-35 significantly reduced the expressions of TXNIP and MAPK phosphorylation compared to the OGD/R group ($P < 0.05$, Figure 5D-5F). Collectively, these data demonstrated that IL-35 inhibited the activation of caspase-1 through regulating the ROS/TXNIP signal pathway.

Discussion

This study confirmed the neuroprotective effects of IL-35 in MCAO mice and OGD/R-induced bEnd.3 cells. In the *in vivo* experiments, IL-35 treatment reduced brain edema, improved neurological deficit, and suppressed BBB breakdown in MCAO-injured mice. In the *in vitro* experiments, IL-35 upregulated the expression of TJ proteins, inhibited the ROS/TXNIP signaling pathway, and suppressed caspase-1 generation in the OGD/R-induced bEnd.3 cells.

Reestablishing blood flow in a tissue previously subject to ischemia, leads to the increased release of pro-inflammatory cytokines, which trigger a series of pathological cascades which will directly or indirectly cause apoptosis, disruption of the BBB, cerebral edema, and hemorrhagic transformation. BBB dysfunction is a key event in the progression of stroke, which is characterized by the following pathophysiological changes: (I) degradation of TJ protein complexes; (II) modulation of endocytosis transport and transport proteins; and (III) inflammatory damage and accumulation of immune cells in brain parenchyma (33).

The molecular characteristics of the BBB primarily involve several transmembrane proteins (such as occludin) and specific accessory proteins (such as ZO-1), which are connected to cytoskeletal filaments (28,34). This report demonstrated that IL-35 treatment significantly reduced EB leakage and improved brain edema in MCAO-injured mice, and reversed the endothelial barrier leakage of bEnd.3 cells injured by OGD/R, suggesting that IL-35 improved the integrity of the BBB.

Caspase-1-mediated EC injury is a key contributor to the pathological process of BBB disruption in ischemic stroke. Inhibition of caspase-1 has been shown to ameliorate ischemia-associated BBB dysfunction and integrity (30,35). In this study, IL-35 treatment inhibited caspase-1-mediated EC injury *in vivo* and *in vitro*. Consistent with these results, previous studies have shown that many Chinese herbal medicines with anti-inflammatory effects (such as hispidulin and ruscogenin) can ameliorate BBB injury after ischemic stroke by markedly suppressing the expression of IL-1 β and cleaved caspase-1 (36,37).

Previous reports have shown that excessive ROS can reverse the interaction between TXNIP and thioredoxin. The released TXNIP then binds the activated inflammasome, leading to enhanced inflammation (16,38). Notably, studies have demonstrated upregulation of the expression of ROS and TXNIP in the brain tissue of MCAO-injured mice (39). This current study verified that IL-35 treatment can reduce the production of ROS, TXNIP, and p38 MAPK expression. Consistent with our results, IL-35 has been shown to inhibit the LPS-induced EC activation via inhibition of the MAPK signaling pathway (19).

There were several limitations to this study. First, we cannot rule out the possibility that IL-35 ameliorates BBB injury after ischemic stroke by targeting other immune cells, such as T helper (Th)17 cells, monocytes, and macrophages. Second, inflammasomes can be activated by multiple mechanisms, such as K⁺ efflux, endoplasmic reticulum (ER) stress, and lysosomal rupture (40). Third, beyond the ROS signaling pathway, GSDMD oxidation serves as a novel mechanism in pyroptotic cell death (41,42). The inhibitory effects of IL-35 on ER stress and amino acid oxidation on GSDMD under oxidative stress warrant further investigation.

This study demonstrated that IL-35 alleviates BBB breakdown and inhibits brain EC injury. The effects of IL-35 in ameliorating the activation of caspase-1 were realized in a ROS/TXNIP-dependent manner, thereby suppressing the disruption of TJ proteins. These findings suggest that

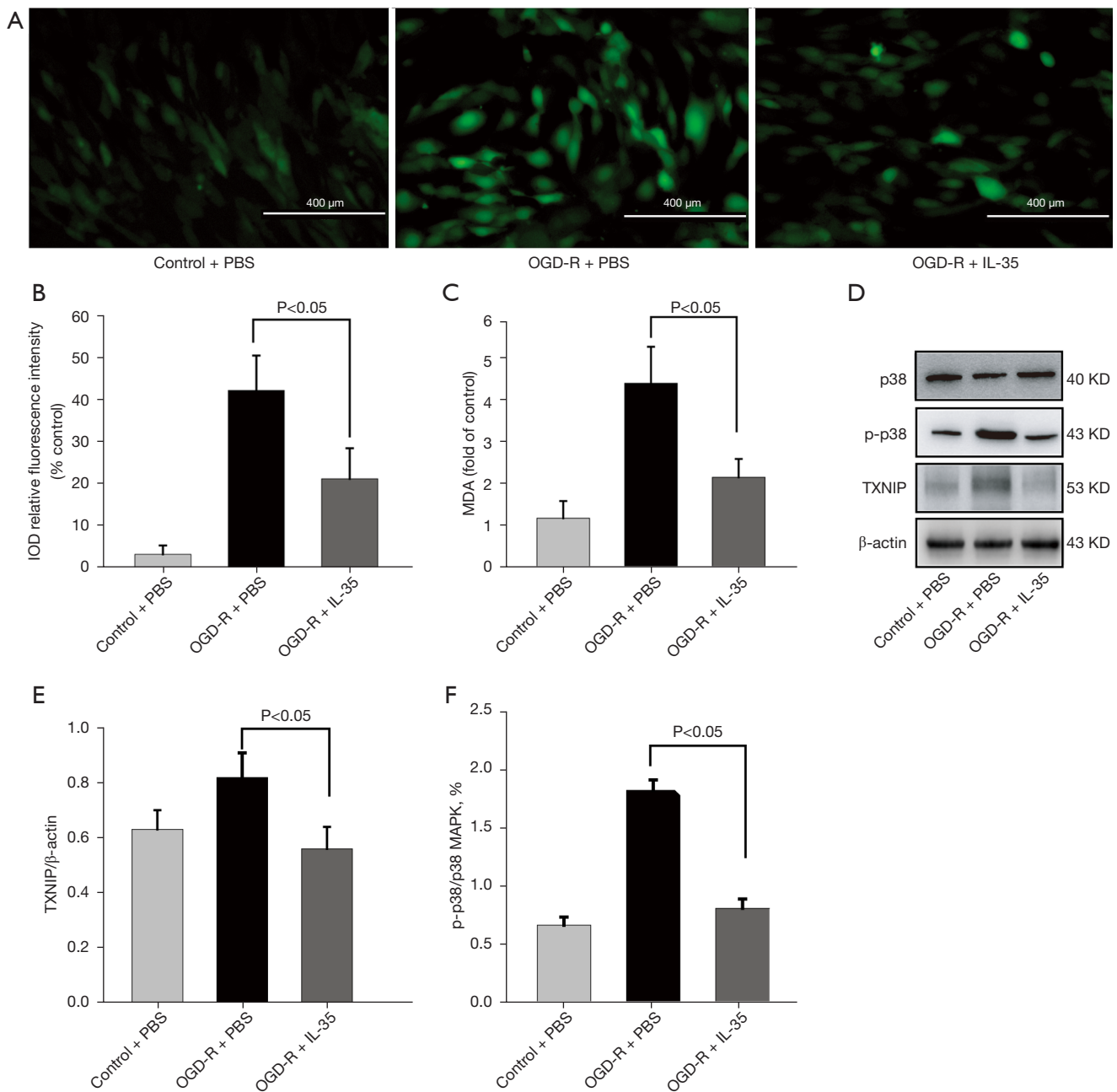


Figure 5 IL-35 suppressed OGD/R-induced ROS generation in endothelial cells. The effects of IL-35 on ROS generation and the MAPK pathway in bEnd.3 cells after 6 hours of OGD and 18 hours reoxygenation. (A) Intracellular ROS was viewed with fluorescence microscopy (scale bar: 400 μ m). (B) The resulting fluorescence intensity was quantified using Image J software. Error bars represent mean \pm SD of at least three independent experiments. (C) The concentration of MDA in cell lysates. (D-F) Representative Western blot bands and quantitative analysis of the ratio of p-p38/p38 and TXNIP. The band intensities were measured using scanning densitometry. Protein expressions were normalized to β -actin (n=3). Data are expressed as mean \pm SD. PBS, phosphate buffered saline; OGD-R, oxygen-glucose deprivation and reperfusion; IL, interleukin; IOD, integrated option density; MDA, malondialdehyde; TXNIP, thioredoxin-interacting protein; ROS, reactive oxygen species; MAPK, mitogen-activated proliferation protein kinase; SD, standard deviation.

IL-35 may have great clinical potential in the treatment of acute cerebral ischemia.

Acknowledgments

Funding: This work was supported by the Jiangsu Province Department of Health, China (Project No. JS2020169).

Footnote

Reporting Checklist: The authors have completed the ARRIVE reporting checklist. Available at <https://atm.amegroups.com/article/view/10.21037/atm-22-2770/rc>

Data Sharing Statement: Available at <https://atm.amegroups.com/article/view/10.21037/atm-22-2770/dss>

Conflicts of Interest: All authors have completed the ICMJE uniform disclosure form (available at <https://atm.amegroups.com/article/view/10.21037/atm-22-2770/coif>). The authors have no conflicts of interest to declare.

Ethical Statement: The authors are accountable for all aspects of the work in ensuring that questions related to the accuracy or integrity of any part of the work are appropriately investigated and resolved. All animal experiments were approved by the Experimental Animal Ethics Committee of Nantong University (Permission No. 2019012) and performed according to *The Guide for the Care and Use of Laboratory Animals* (National Institutes of Health Publication).

Open Access Statement: This is an Open Access article distributed in accordance with the Creative Commons Attribution-NonCommercial-NoDerivs 4.0 International License (CC BY-NC-ND 4.0), which permits the non-commercial replication and distribution of the article with the strict proviso that no changes or edits are made and the original work is properly cited (including links to both the formal publication through the relevant DOI and the license). See: <https://creativecommons.org/licenses/by-nc-nd/4.0/>.

References

1. Feske SK. Ischemic Stroke. *Am J Med* 2021;134:1457-64.
2. Paul S, Candelario-Jalil E. Emerging neuroprotective strategies for the treatment of ischemic stroke: An overview of clinical and preclinical studies. *Exp Neurol* 2021;335:113518.
3. Sarvari S, Moakedi F, Hone E, et al. Mechanisms in blood-brain barrier opening and metabolism-challenged cerebrovascular ischemia with emphasis on ischemic stroke. *Metab Brain Dis* 2020;35:851-68.
4. Maida CD, Norrito RL, Daidone M, et al. Neuroinflammatory Mechanisms in Ischemic Stroke: Focus on Cardioembolic Stroke, Background, and Therapeutic Approaches. *Int J Mol Sci* 2020;21:6454.
5. Yawoot N, Govitrapong P, Tocharus C, et al. Ischemic stroke, obesity, and the anti-inflammatory role of melatonin. *Biofactors* 2021;47:41-58.
6. Orellana-Urzúa S, Rojas I, Líbano L, et al. Pathophysiology of Ischemic Stroke: Role of Oxidative Stress. *Curr Pharm Des* 2020;26:4246-60.
7. Franke M, Bieber M, Kraft P, et al. The NLRP3 inflammasome drives inflammation in ischemia/reperfusion injury after transient middle cerebral artery occlusion in mice. *Brain Behav Immun* 2021;92:223-33.
8. Gong S, Cao G, Li F, et al. Endothelial Conditional Knockdown of NMMHC IIA (Nonmuscle Myosin Heavy Chain IIA) Attenuates Blood-Brain Barrier Damage During Ischemia-Reperfusion Injury. *Stroke* 2021;52:1053-64.
9. Jiang M, Li R, Lyu J, et al. MCC950, a selective NLRP3 inflammasome inhibitor, improves neurologic function and survival after cardiac arrest and resuscitation. *J Neuroinflammation* 2020;17:256.
10. Burdette BE, Esparza AN, Zhu H, et al. Gasdermin D in pyroptosis. *Acta Pharm Sin B* 2021;11:2768-82.
11. Liu X, Zhang Z, Ruan J, et al. Inflammasome-activated gasdermin D causes pyroptosis by forming membrane pores. *Nature* 2016;535:153-8.
12. Wang H, Chen H, Jin J, et al. Inhibition of the NLRP3 inflammasome reduces brain edema and regulates the distribution of aquaporin-4 after cerebral ischaemia-reperfusion. *Life Sci* 2020;251:117638.
13. Ren S, Wu G, Huang Y, et al. MiR-18a Aggravates Intracranial Hemorrhage by Regulating RUNX1-Occludin/ZO-1 Axis to Increase BBB Permeability. *J Stroke Cerebrovasc Dis* 2021;30:105878.
14. Zhang A, Lu Y, Yuan L, et al. miR-29a-5p Alleviates Traumatic Brain Injury- (TBI-) Induced Permeability Disruption via Regulating NLRP3 Pathway. *Dis Markers* 2021;2021:9556513.
15. Dai Y, Wang S, Chang S, et al. M2 macrophage-derived exosomes carry microRNA-148a to alleviate myocardial ischemia/reperfusion injury via inhibiting TXNIP and

- the TLR4/NF-kappaB/NLRP3 inflammasome signaling pathway. *J Mol Cell Cardiol* 2020;142:65-79.
16. Tsubaki H, Tooyama I, Walker DG. Thioredoxin-Interacting Protein (TXNIP) with Focus on Brain and Neurodegenerative Diseases. *Int J Mol Sci* 2020;21:9357.
 17. Feng YS, Tan ZX, Wang MM, et al. Inhibition of NLRP3 Inflammasome: A Prospective Target for the Treatment of Ischemic Stroke. *Front Cell Neurosci* 2020;14:155.
 18. Yazdani Z, Rafiei A, Golpour M, et al. IL-35, a double-edged sword in cancer. *J Cell Biochem* 2020;121:2064-76.
 19. Li M, Liu Y, Fu Y, et al. Interleukin-35 inhibits lipopolysaccharide-induced endothelial cell activation by downregulating inflammation and apoptosis. *Exp Cell Res* 2021;407:112784.
 20. Shao Y, Yang WY, Saaoud F, et al. IL-35 promotes CD4+Foxp3+ Tregs and inhibits atherosclerosis via maintaining CCR5-amplified Treg-suppressive mechanisms. *JCI Insight* 2021;6:152511.
 21. Li M, Qian L, Yu J, et al. Interleukin-35 inhibits human umbilical vein endothelial cell injury induced by sera from pre-eclampsia patients by up-regulating S100A8 protein expression. *Hypertens Pregnancy* 2020;39:126-38.
 22. Correale J, Marrodan M, Carnero Contentti E. Interleukin-35 is a critical regulator of immunity during helminth infections associated with multiple sclerosis. *Immunology* 2021;164:569-86.
 23. Srivastava P, Cronin CG, Scranton VL, et al. Neuroprotective and neuro-rehabilitative effects of acute purinergic receptor P2X4 (P2X4R) blockade after ischemic stroke. *Exp Neurol* 2020;329:113308.
 24. Xu C, Zhu H, Shen R, et al. IL-35 is a Protective Immunomodulator in Brain Ischemic Injury in Mice. *Neurochem Res* 2018;43:1454-63.
 25. Yang X, Wu S. N-oleoylethanolamine - phosphatidylcholine complex loaded, DSPE-PEG integrated liposomes for efficient stroke. *Drug Deliv* 2021;28:2525-33.
 26. Chen J, Yang L, Geng L, et al. Inhibition of Acyl-CoA Synthetase Long-Chain Family Member 4 Facilitates Neurological Recovery After Stroke by Regulation Ferroptosis. *Front Cell Neurosci* 2021;15:632354.
 27. Liu X, Zhang M, Liu H, et al. Bone marrow mesenchymal stem cell-derived exosomes attenuate cerebral ischemia-reperfusion injury-induced neuroinflammation and pyroptosis by modulating microglia M1/M2 phenotypes. *Exp Neurol* 2021;341:113700.
 28. Kim KA, Kim D, Kim JH, et al. Autophagy-mediated occludin degradation contributes to blood-brain barrier disruption during ischemia in bEnd.3 brain endothelial cells and rat ischemic stroke models. *Fluids Barriers CNS* 2020;17:21.
 29. Benz F, Liebner S. Structure and Function of the Blood-Brain Barrier (BBB). *Handb Exp Pharmacol* 2022;273:3-31.
 30. Liang Y, Song P, Chen W, et al. Inhibition of Caspase-1 Ameliorates Ischemia-Associated Blood-Brain Barrier Dysfunction and Integrity by Suppressing Pyroptosis Activation. *Front Cell Neurosci* 2020;14:540669.
 31. Dai X, Liao R, Liu C, et al. Epigenetic regulation of TXNIP-mediated oxidative stress and NLRP3 inflammasome activation contributes to SAHH inhibition-aggravated diabetic nephropathy. *Redox Biol* 2021;45:102033.
 32. Dong R, Xue Z, Fan G, et al. Pin1 Promotes NLRP3 Inflammasome Activation by Phosphorylation of p38 MAPK Pathway in Septic Shock. *Front Immunol* 2021;12:620238.
 33. Gu M, Mei XL, Zhao YN. Sepsis and Cerebral Dysfunction: BBB Damage, Neuroinflammation, Oxidative Stress, Apoptosis and Autophagy as Key Mediators and the Potential Therapeutic Approaches. *Neurotox Res* 2021;39:489-503.
 34. Rom S, Heldt NA, Gajghate S, et al. Hyperglycemia and advanced glycation end products disrupt BBB and promote occludin and claudin-5 protein secretion on extracellular microvesicles. *Sci Rep* 2020;10:7274.
 35. Gu L, Sun M, Li R, et al. Didymin Suppresses Microglia Pyroptosis and Neuroinflammation Through the Asc/Caspase-1/GSDMD Pathway Following Experimental Intracerebral Hemorrhage. *Front Immunol* 2022;13:810582.
 36. Zhai K, Mazurakova A, Koklesova L, et al. Flavonoids Synergistically Enhance the Anti-Glioblastoma Effects of Chemotherapeutic Drugs. *Biomolecules* 2021;11:1841.
 37. Zhang Y, Hu Y, Li M, et al. The Traditional Chinese Medicine Compound, GRS, Alleviates Blood-Brain Barrier Dysfunction. *Drug Des Devel Ther* 2020;14:933-47.
 38. Zhang M, Hu G, Shao N, et al. Thioredoxin-interacting protein (TXNIP) as a target for Alzheimer's disease: flavonoids and phenols. *Inflammopharmacology* 2021;29:1317-29.
 39. Yao Y, Hu S, Zhang C, et al. Ginsenoside Rd attenuates cerebral ischemia/reperfusion injury by exerting an anti-pyroptotic effect via the miR-139-5p/FoxO1/Keap1/Nrf2 axis. *Int Immunopharmacol* 2022;105:108582.
 40. Zhou Y, Tong Z, Jiang S, et al. The Roles of Endoplasmic Reticulum in NLRP3 Inflammasome Activation. *Cells*

- 2020;9:1219.
41. Jia Y, Cui R, Wang C, et al. Metformin protects against intestinal ischemia-reperfusion injury and cell pyroptosis via TXNIP-NLRP3-GSDMD pathway. *Redox Biol* 2020;32:101534.

42. Fidler TP, Xue C, Yalcinkaya M, et al. The AIM2 inflammasome exacerbates atherosclerosis in clonal haematopoiesis. *Nature* 2021;592:296-301.

(English Language Editor: J. Teoh)

Cite this article as: Qian L, Li M, Lin X, Teng H, Yu L, Jiang M. Interleukin-35 attenuates blood-brain barrier dysfunction caused by cerebral ischemia-reperfusion injury through inhibiting brain endothelial cell injury. *Ann Transl Med* 2022;10(14):776. doi: 10.21037/atm-22-2770